EUROFUSION WPMAT-CP(16) 16503

H. Gietl et al.

Material qualification of tungsten fibre-reinforced tungsten composite by means of tension

Preprint of Paper to be submitted for publication in Proceedings of 29th Symposium on Fusion Technology (SOFT 2016)

This work has been carried out within the framework of the EUROfusion Consortium and has received funding from the Euratom research and training programme 2014-2018 under grant agreement No 633053. The views and opinions expressed herein do not necessarily reflect those of the European Commission.

Material qualification of tungsten fibre-reinforced tungsten composits by means of tension test - monotonic test in as-fabricated condition

H. Gietl[a,b], J. Riesch[a], J.W. Coenen[c], T. Höschen[a], Ch.Linsmeier[c], R.Neu[a,b]

[a] *Max-Planck-Institut für Plasmaphysik, 85748 Garching, Germany*
[b] *Technische Universität München, Boltzmannstrasse 15, 85748 Garching, Germany*
[c] *Forschungszentrum Jülich GmbH, Institut fuer Energie und Klimaforschung, Partner of the Trilateral Euregio Cluster (TEC), 52425 Juelich, Germany*

Abstract

To overcome the inherent brittleness of tungsten, which is a promising candidate for a plasma-facing material in a future fusion device, tungsten fibre-reinforced tungsten composits (W_f/W) have been developed. As a part of the materials qualification program, we present in this contribution the results of monotonic tension tests on W_f/W. The material parameters were evaluated by means of displacement controlled tension tests. The tests give insight on the ultimate tensile strength and reveal the active toughening mechanisms under tension load within the composite. In the as-fabricated condition the material is still able to bear rising loads despite multiple matrix cracks. Fibre necking as well as fibre pull out was observed leading to the typical pseudo ductile behaviour of the composite. The description of the mechanical tests is supplemented by detailed microstructural investigations.

Keywords: tungsten, fibre-reinforced composite, tension test, ultimate tensile strength

1. Introduction

Tungsten is a promising plasma-facing material for future fusion reactors due to its unique property combination such as a low sputter yield, a high melting point and a low activation [1]. The main drawbacks for the use of pure tungsten are its brittleness below the ductile-to-brittle transition temperature [2, 3, 4] and the embrittlement during operation e.g. by overheating and/or neutron irradiation [5, 6, 7]. These limitations are mitigated by using tungsten fibre-reinforced tungsten composite (W_f/W) which utilizes extrinsic mechanisms to improve the toughness similar to ceramic fibre-reinforced ceramics [8]. It was shown that this idea in principle works in the as-fabricated [9] as well as in the embrittled material [10]. The fibres are made of W wire which was characterized in detail by means of tension tests [11, 12, 13]. Recently a layered chemical vapour deposition process was developed allowing the production of large and reproducible samples [14]. This allowed then the launch of an extended material qualification program in which three point bending test have been performed in a first step. In Charpy impact tests it was proven that the toughening effect is still working under high deformation rates [14]. In this paper we are presenting the next step in this program, the behaviour of W_f/W under tension load which is in general seen as the most critical load for brittle material. The ultimate tensile strength (UTS) of W_f/W as a normalized material parameter and the detailed microstructural investigations would in addition be very helpful for the further development of W_f/W based structures.

2. Materials and Experimental Procedure

The raw material was produced as a plate with a layered chemical vapor deposition (CVD) process performed at Archer Technicoat Ltd. (High Wycombe, UK). A detailed process description is given in [14]. The preform of a single layer was a unidirectional fibre arrangement consisting of pure tungsten wires with a diameter of 150 μm. This preform was coated with 1 μm thick interlayer of Er_2O_3 by magnetron sputtering. The CVD process is a layer-wise process and thereby it can be split into three process steps. At first the preform needs to be placed on a heating plate inside the process chamber. Then tungsten is deposited to create a solid material. In the last step, the whole process chamber is opened to place the next preform layer on top of the already coated solid composite. For the material used in this experiments a overall thickness of 3 mm (10 layers) W_f/W was produced. The fibre volume ratio of the specimens was 21% and the overall density was 92.5%. Out of this material tension specimens were manufactured with electrical discharge machining (EDM) according to the geometry shown in Fig. 1. The measuring length of the specimen was 16.5 mm.

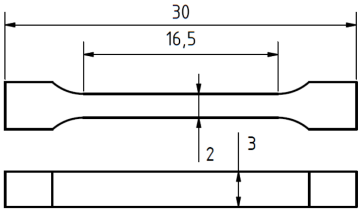

Figure 1: Dimensions of specimen for tension tests

The tension tests were performed with a universal testing device (TIRAtest 2820, Nr. R050/01, Fa. TIRA GmbH). The load was recorded by a 20 kN load cell. A specially designed holding system was used to avoid stress peaks at the contact surface of the holder and the specimen. Moreover, the holders were mounted with a chain system to the universal testing device to ensure a uni-axial stress state within the specimen (Fig. 2).

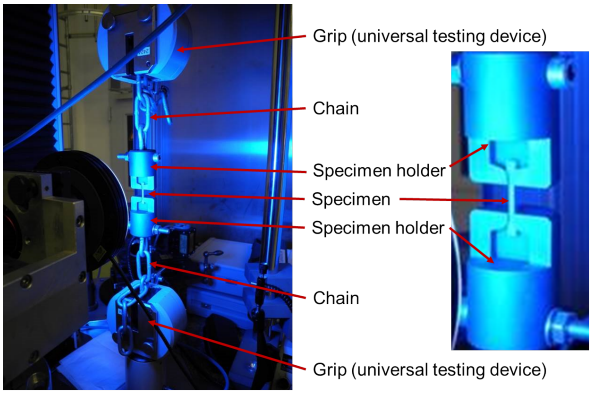

Figure 2: Experimental setup for tension tests

Each specimen was preloaded with 20 N and the test was conducted at room temperature with a constant displacement rate of 10 μm/s.
After the test, the fractured surfaces and the polished cross section were investigated by scanning electron microscopy (SEM), confocal laser scanning microscopy (CLSM) and optical microscopy. In total two samples were tested in a monotonic tension test (specimen 1 and 2).

3. Results

The stress-strain curves of two tests are shown in Fig. 3. Although both specimens were preloaded with 20 N before the tensile test, both stress-strain curves show at the beginning a nonlinear behaviour due to the setting of the system before the load is fully transferred into the specimen.
The ultimate tensile strength (UTS) of specimen 1 is 482 MPa and 557 MPa of specimen 2. The stress-strain curve of specimen 1 shows a first drop at 80 MPa and a first drop of specimen 2 is shown at 125 MPa. This indicates the first crack in the matrix material. In total 19 crack events are observed for specimen 1 and 12 crack events for specimen 2. For Specimen 1 a load drop to around 100 MPa was measured but the specimen is still able to withstand that load before full failure. After reaching the UTS of specimen 2 a slight decrease in stress to 500 MPa is detected followed ba an abrupt failure.
The fracture surface of specimen 1 is shown in Fig. 4. The fibre layer which was grown at first is on the left side of Fig. 4 a). The fracture surfaces has four steps which can be seen in the side view (Fig. 5). The first step includes six fibre layers and has the largest area. The second and third step consists of one fibre layer and the fourth step contain two fibre layers. The height difference from step one to two is 1.23 mm, from two to three is 0.81 mm, and from three to four the step is 5.14

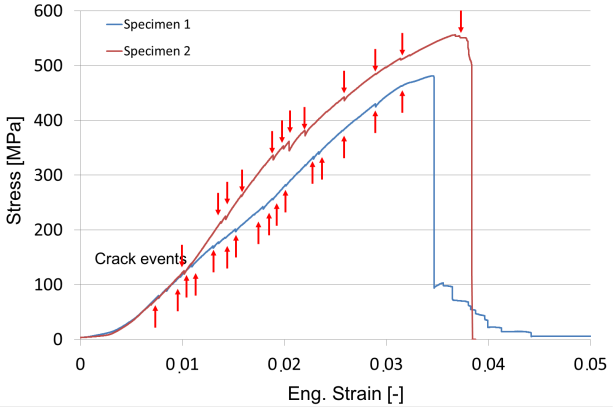

Figure 3: Stress-strain curves for the specimens 1 and 2

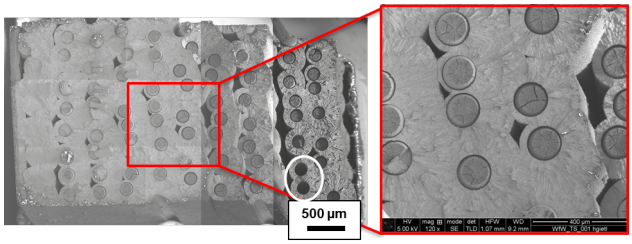

Figure 4: SEM image of the fracture surface specimen 1

mm. In step one very few pores can be seen and these pores are distributed over the whole area. The pores are located between the layers. The porosity in this area is 2.2% (density: 97.8%). Large pores are located between the layers where as the largest is between step 3 and 4.

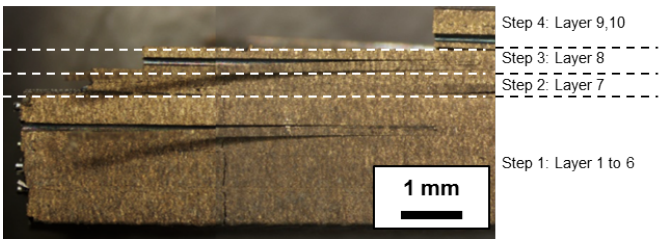

Figure 5: Side view of the ruptured specimen 1

A total amount of 77 fibres contribute to the tensile strength of this specimen. It is found that ~ 80% of the fibres show a ductile behaviour and the rest failed in a brittle manner. Most of the brittle fibres were in the first layer.

The SEM images in Fig. 6 shows the fracture surfaces of the specimen 2. This fracture area has two steps and the height difference between the two steps is 1.92 mm. The first step consists of one fibre layer and within this layer no pores are visible. However, between layer one and layer two pores with a elongated shape can be seen. The second step which consists of eight fibre layers has no large pores only small and they are located between the fibre layers. The porosity for this area is below 1.9% (density: 98.1%).

This specimen has 74 fibres and over 94% behave ductile. Again most of the brittle fibres are in the first layer of fibres.

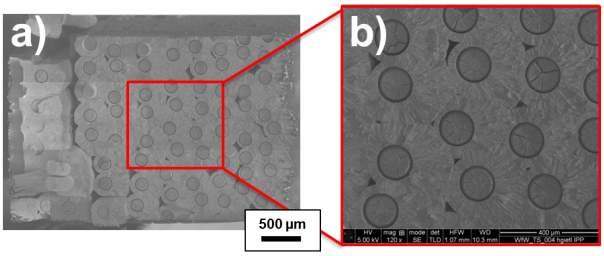

Figure 6: SEM image of the fracture surface specimen 2

In Table 1 the total amount of fibres as well as the number of fibres which show ductile and brittle behaviour are presented for both specimens.

Table 1: Number of fibres in the specimens

Fibres	total	ductile	brittle
Specimen 1	77	61	16
Specimen 2	74	70	4

The second half of the ruptured specimen 1 is shown in Fig. 7. In Fig. 7 a) two cracks are observed beside the already discussed steps. Two fibres which stick out of the composite indicates a massive fibre pull-out. The corresponding site of the pull-out can be seen in Fig. 4 and is marked with a white circle. The specimen was polished in a way that one fibre was cut in half. A slight of axis-angle during polishing lead to a variation in the fibre diameter visible in Fig. 7 c). Fig. 7 b) shows the detailed cross section of that fibre. The matrix is cracked six times over the shown fibre length. These cracks are evenly distributed and show different openings. The largest crack has a width of 45 μm (Fig. 7 d), Fig. 7 d)). Only on the fractured surface (Fig. 7 e)) the fibre shows a ductile deformation.
Fig. 7 f) shows a detailed view of a crack region where the interlayer, the fibre and matrix is visible. The debonding of the interlayer is shown and is detected between interlayer and fibre. So it can be seen that the interlayer sticks to the matrix and not to fibre.

4. Discussion

As it was shown in the fracture surfaces of the specimens different steps during failure are observed. These fracture steps mainly occur between two different deposition layers and are most probably caused by the weak bonding of some layers to the neighbouring layer. Two reasons for that can be identified. The first is the layer-wise production process and the second is the fibre preform arrangement. These layered deposition process faces the problem that the vacuum chamber needs to be opened for placing the next fibre layer. This can lead to impurities on the surface which lead to a weak and undefined bonding. The second reason are the pores which also weaken the bonding. The reasons for these pores can be found in the fibre arrangement technique. This was for that sample a mainly handmade process which causes at some points inaccuracies of the fibre placement. This produces during the deposition step a blocking structure and no WF_6 can pass through that structure and no tungsten is deposited on that interface.

Brittle fibre have a much lower strength compared to there ductile counterparts [14]. Assuming that only the fibres failed in a ductile manner are contributing to the ultimate strength (the matrix has already failed) a theoretical UTS for a single fibre can be calculated as follows.

$$\sigma_{\text{fibre}} = F_{W_f/W} \,/\, A_{\text{all ductile fibres}}$$

This leads to a theoretical fibre stength of 2680 MPa for specimen 1 and 2700 MPa for specimen 2. Zhao et al. [11] found the UTS of similar fibres to be 2926.0 ± 1.5 MPa. This good agreement supports our assumption that the UTS is dominated by she fibres.

Specimen 1 is able to withstand 100 MPa after a massive load drop before full failure. A reason for that might be the massive pull out observed for two fibres. This could be a hint that pull-out might pose a significant contribution to the toughening. Further investigations are necessary.

Multiple matrix cracking is observed with comparable crack spacings. This was expected for W_f/W [15] and is also well known for brittle matrix composites where the matrix has a lower failure strain than the fibre [16, 17]. In contrast to the expectation in [15] no multiple necking for a single fibre has been observed. Nerveless a plastic deformation of the fibre over the whole length is possible. The necking of the fibre is the last step of the deformation process and takes place nearly at the failure of a singe fibre [12]. A possible reason is that the bonding between the fibre (and matrix) is to weak in order to reach the yield point of the fibres in multiple locations. The interlayer is a key factor in the toughening for the toughening mechanisms. It must be strong enough to transfer the load from the matrix to fibre. It is also necessary that it debonds or fractures at a stress which is before the fracture of the fibre. If it does not debond the fibres would just fail and the material would fail like a brittle material [18, 19]. On the other hand if the interlayer bonding is to week the stress can not be transferred from the matrix to the fibre and multiple matrix cracking can not emerge. With such an optimized interlayer more fibres of the composite would fail ductile which leads to an increased fracture toughness [15]. For Er_2O_3 as an interlayer it is seen that the debonding takes place between the fibre and the interlayer. That is because the interlayer is a ceramic material with a lower failure strain than the ductile fibre. So the interlayer behaviour is comparable with the brittle tungsten matrix. This failure is beneficial for the sliding of the fibres and leads to the pull-out of the fibre [19].

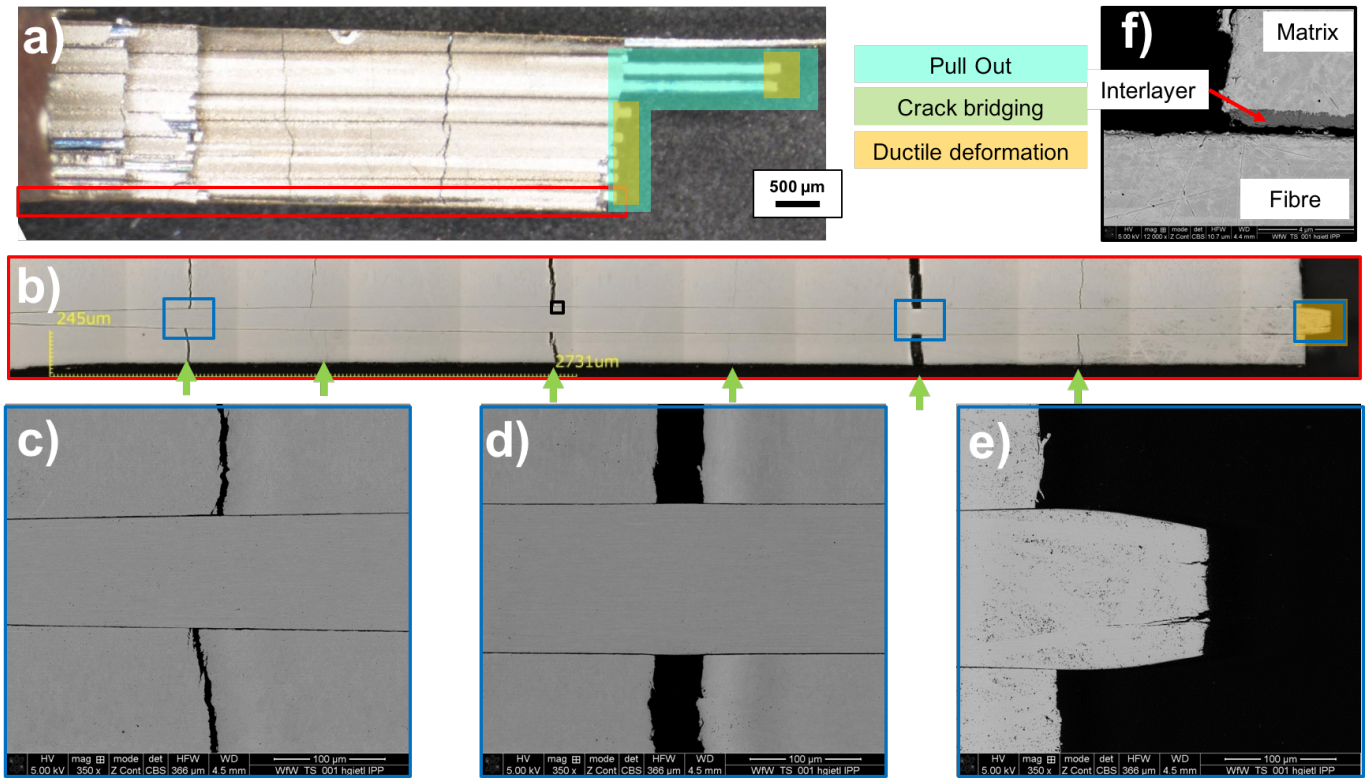

Figure 7: Detailed view specimen 1 (a) optical microscope image, b) CLSM image, c), d), e), and f) SEM images)

5. Conclusion and Outlook

For the first time pseudo ductile behaviour was demonstrated with a bulk W_f/W. The stress strain diagram of the tensile correspond to the curves which are well known from literature for pseudo ductile behaviour of composite materials [20]. Most of the fibres fail ductile during a tension test and the fibre strength could be calculated out of the UTS of the specimens. Furthermore, only one ductile failure, the UTS and multiple matrix cracking could be demonstrated for the first time in W_f/W. It could also be demonstrated that fibre pull-out can pose a significant contributen.

At a next step at the material qualification program a cyclic loading test are used to get insight into the fatigue behaviour of W_f/W. In addition a optimized manufacture routine for producing the tungsten matrix is under development at the moment. Moreover, new interface materials and new testing methods are under investigation to maximize the energy dissipation and do influence the bulk behaviour.

Acknowledgement

The authors want to acknowledge the Osram GmbH, Schwabmünchen, Germany for providing the tungsten wire, Archer Technicoat Ltd, High Wycombe, UK for assistance in the CVD production and the whole W_f/W team. This work has been carried out within the framework of the EUROfusion Consortium and has received funding from the Euratom research and training programme 2014-2018 under grant agreement No 633053. The views and opinions expressed herein do not necessarily reflect those of the European Commission.

References

[1] J.W. Coenen, S. Antusch, M. Aumann, W. Biel, J. Du, J. Engels, S. Heuer, A. Houben, T. Hoeschen, B. Jasper, F. Koch, J. Linke, A. Litnovsky, Y. Mao, R. Neu, G. Pintsuk, J. Riesch, M. Rasinski, J. Reiser, M. Rieth, A. Terra, B. Unterberg, Th. Weber, T. Wegener, J-H. You, and Ch. Linsmeier. Materials for DEMO and reactor applications boundary conditions and new concepts. *Physica Scripta*, T167:014002, 2016.

[2] C. Gandhi and M.F. Ashby. Overview no. 5: Fracture-mechanism maps for materials which cleave: F.C.C., B.C.C. and H.C.P. metals and ceramics. *Acta Metallurgica*, 27(10):1565–1602, 1979.

[3] E. Lassner and W.-D. Schubert. *Tungsten - Properties, Chemistry, Technology of the Element, Alloys, and Chemical Compound*. Springer, 1999.

[4] J. Reiser, M. Rieth, B. Dafferner, and A. Hoffmann. Charpy impact properties of pure tungsten plate material in as-received and recrystallized condition. *Journal of Nuclear Materials*, 442:204–207, 2013.

[5] W. Yih and C. Wang. *Tungsten: Sources, Metallurgy, Properties, and Applications*. Springer US, 1979.

[6] V. Barabash, G. Federici, M. Rödig, L. Snead, and C. Wu. Neutron irradiation effects on plasma facing materials. *Journal of Nuclear Materials*, 283-287:138–146, 2000.

[7] J.M. Steichen. Tensile properties of neutron irradiated TZM and tungsten. *Journal of Nuclear Materials*, 60:13–19, 1976.

[8] A.G. Evans. Perspective on the development of high-toughness ceramics. *Journal of American Ceramic Society*, 73:187–206, 1990.

[9] J. Riesch, T. Höschen, Ch Linsmeier, S. Wurster, and J.-H. You. Enhanced toughness and stable crack propagation in a novel tungsten fibre-reinforced tungsten composite produced by chemical vapour infiltration. *Physica Scripta*, T159:014031, 2014.

[10] R. Neu, J. Riesch, Coenen J.W., J. Brinkmann, A. Calvo, S. Elgeti, C. Garcia-Rosales, H. Greuner, T. Hschen, G. Holzner, F. Klein, F. Koch, Ch. Linsmeier, A. Litnovsky, T. Wegener, S. Wurster, and J-H. You. Advanced tungsten materials for plasma-facing components of DEMO and fusion power plants. *Fusion Engineering and Design*, 109-111: Part A:1046–1052, 2016.

[11] P. Zhao, J. Riesch, T. Höschen, J. Almannstötter, M. Balden, J.W. Coenen, U. Himml, U. von Toussaint, and R. Neu. Microstructure, mechanical behavior and fracture of pure tungsten wires after different heat treatments. *International Journal of Refractory Metals and Hard Materials*, in preperation, 2016.

[12] J. Riesch, J. Almannstötter, J.W. Coenen, M. Fuhr, H. Gietl, Y. Han, T. Höschen, Ch. Linsmeier, N. Travitzky, and P. Zhao. Properties of drawn w wire used as high performance fibre in tungsten fibre-reinforced tungsten composite. *IOP Conference Series: Materials Science and Engineering*, 136:012043, 2016.

[13] J. Riesch, Y. Han, J. Almannstötter, Coenen J.W., T. Höschen, B. Jasper, P. Zhao, Ch. Linsmeier, and R. Neu. Development of tungsten fibre-reinforced tungsten composites towards their use in DEMO - potassium doped tungsten wire. *Physica Scripta*, T167:014006, 2016.

[14] J. Riesch, M. Aumann, J.W. Coenen, H. Gietl, G. Holzner, T. Höschen, P. Huber, M. Li, Ch. Linsmeier, and R. Neu. Chemically deposited tungsten fibre-reinforced tungsten - the way to a mock-up for divertor applications. *Nuclear Materials and Energy*, In Press, 2016.

[15] J. Riesch, J.Y. Buffiere, T Höschen, M. di Michiel, M. Scheel, Ch. Linsmeier, and J.-H. You. In situ synchrotron tomography estimation of toughening effect by semi-ductile fibre reinforcement in a tungsten-fibre-reinforced tungsten composite system. *Acta Materialia*, 61:7060–7071, 2013.

[16] W.A. Curtin. Multiple matrix cracking in brittle matrix composites. *Acta Metallurgica et Materialia*, 41(5):1369–1377, 1993.

[17] X.F. Yang and K.M. Knowles. The one-dimensional car parking problem and its application to the distribution of spacings between matrix cracks in unidirectional fiber-reinforced brittle materials. *Journal of the American Ceramic Society*, 75(1):141–147, 1992.

[18] M.-Y. He and J. W. Hutchinson. Crack deflection at an interface between dissimilar elastic materials. *International Journal of Solids and Structures*, 25:1053–1067, 1989.

[19] A.G. Evans, F.W. Zok, and J. Davis. The role of interfaces in fiber-reinforced brittle matrix composites. *Composites Science and Technology*, 42:3–24, 1991.

[20] K. K. Chawla. *Ceramic Matrix Composites*. Springer US, 2001.